JOC*Note*

Inter- and Intramolecular-Bridge-Mediated Electron Transfer in Aliphatic Halides

Jorge G. Uranga, D. Mariano A. Vera, Ana N. Santiago, and Adriana B. Pierini*

INFIQC − Departamento de Química Orgánica, Facultad de Ciencias Químicas, Universidad Nacional de Córdoba, Ciudad Universitaria, 5000 Córdoba, Argentina

adriana@dqo.fcq.unc.edu.ar

Received January 10, 2006

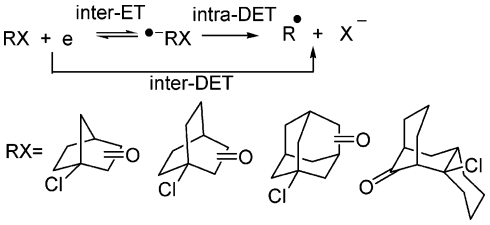

The anionic surfaces of the 1-chloro- and 4-chlorobicyclo-[2.2.1]heptan-2-one, 1-chloro- and 4-chlorobicyclo[2.2.2]-octan-2-one, 1-chloro- and 5-chloroadamantan-2-one, and 2-chlorotricyclo[7.3.1.0^{2,7}]tridecan-13-one were explored using DFT functionals with full geometry optimization in solution. The reductive cleavage of these compounds is controlled by the rigidity of the polycycle, its capability to form an unstrained radical, and by the relative carbonyl/C−Cl disposition on the bridge. Such control can be exerted by either a concerted-dissociative or a stepwise mechanism with radical anions as intermediates. 5-Chloroadamantan-2-one is the most suitable compound to follow the latter pathway.

The final outcome of an intermolecular electron transfer (ET) reaction to organic halides is the formation of radicals by dissociation of the C−halogen (C−X) bond. This reaction may follow either a concerted-dissociative pathway by which the C−X bond breaks as the electron is being transferred (Figure 1b) or a stepwise mechanism, with radical anions (RAs) as intermediates (Figure 1a).[1] The stepwise mechanism is the preferred pathway followed by halides bearing a π acceptor of low enough energy to accommodate the incoming electron.[1,2] The presence of RAs has been clearly established in many organic reactions, among them the $S_{RN}1$ radical chain mechanism, with which we are also experimentally concerned,[3] as well as in many electrochemical[2] and biological processes such as, for example, DNA damage.[4]

In these intermediates, the π acceptor (πAc) can be linked to the C−X bond through a bridge or can be orthogonal and adjacent to it, as in the case of aromatic halides. For these

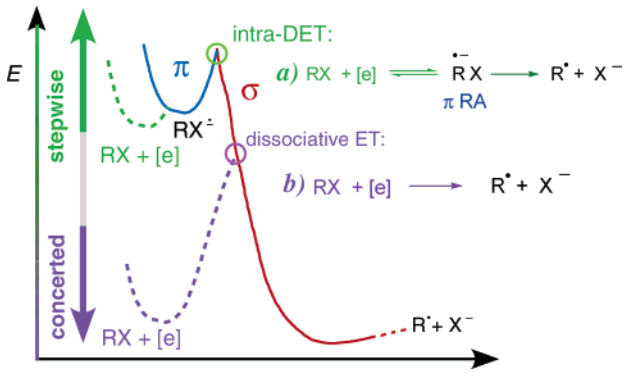

FIGURE 1. Profiles for the ET to RX (R = Ar, πAc-alkyl). The reaction can switch from (a) stepwise to (b) concerted, depending on $\Delta G_{RX^{\bullet-}\rightarrow R^{\bullet}+X^{-}}$ and the driving force offered by the electron donor [e]. Adapted from ref 1, 6.

compounds, two different anionic surfaces are a priori possible, one corresponding to a RA with the extra electron located on the π system (πRA) and the other corresponding to the σ* C−X anionic surface. The dissociation of these species is interpreted as the result of an intramolecular-dissociative ET (intra-DET) from the π to the σ* C−X subsystem (Figure 1, eq a). The existence of a πRA does not necessarily imply a stepwise reductive cleavage as the pathway followed under homogeneous or heterogeneous ET conditions depends on the standard free energy for cleavage of the RA and the driving force offered by the electron donor (Figure 1).[1,5]

Previously, we have carried out a thorough study of the reactivity of adjacent $\pi-\sigma$ systems showing on molecular bases that, besides the relative stability of both surfaces, other factors such as their topology, the $\pi-\sigma$ crossing coordinate, the electronic and geometric properties of the different anionic systems, and the different extent to which a polar solvent stabilizes them should be taken into account to understand the overall process (Figure 1).[6]

Here, we will present the study of anionic species in which the π and σ subsystems are separated by aliphatic bridges. In this aim, we choose the set of bridges of different flexibility presented in Chart 1 keeping the carbonyl group as πAc and X = Cl as leaving group (methyl substituents were not included in the calculations). For these compounds, apart from the factors that mediate the $\pi-\sigma$ interconversion in adjacent aryl systems, the extent of their separation and the structural and electronic properties of the bridge are also expected to influence the rate of the dissociation.

The subfamilies of compounds **1** and **3** have experienced π catalysis, measured by competition experiments of pairs of compounds against Ph_2P^- ions as nucleophile.[7a,b] Different from that observed for **1** and **3**, the π substitution at C_γ leads to a decrease in reactivity in the adamantyl system (**2**).[7c] The same trend has also been observed toward Me_3Sn^- ions.[7c] The relative reactivity determined follows the order[7] **1a** ≈ **3a** ≪ **1c** ≈ **3b** < **1b** with $k_{\mathbf{1b}} = 2.8 \times k_{\mathbf{1c}}$ and $k_{\mathbf{3b}} = 1.1 \times k_{\mathbf{1c}}$ (against Ph_2P^-

(1) Savéant, J.-M. In *Advances in Physical Organic Chemistry*; Tidwell, T. T., Ed.; Academic Press: New York, 2000; p 35.
(2) Savéant, J.-M. *Adv. Phys. Org. Chem.* **1990**, *26*, 1.
(3) (a) Rossi, R. A.; Pierini, A. B.; Peñéñory, A. B. *Chem. Rev.* **2003**, *103*, 71. (b) Rossi, R. A.; Pierini, A. B.; Santiago, A. N. In *Organic Reactions*; Paquette, L. A., Bittman, R., Eds.; John Wiley & Sons: New York, 1999; p 1.
(4) (a) Borosky, G. L.; Nishimoto, S.-I.; Pierini, A. B. *THEOCHEM* **2000**, *499*, 151. (b) Wetmore, S. D.; Boyd, R. J.; Eriksson, L. A. *Chem. Phys. Lett.* **2001**, *343*, 151. (c) Laage, D.; Burghart, I.; Sommerfeld, T.; Hynes, J. T. *ChemPhysChem* **2003**, *4*, 61.
(5) Besides ref 1, some representative references on the subject: (a) Andrieux, C. P.; Robert, M.; Saeva, F. D.; Savéant, J.-M. *J. Am. Chem. Soc.* **1994**, *116*, 7864. (b) Antonello, S.; Maran, F. *J. Am. Chem. Soc.* **1997**, *119*, 12595. (c) Pause, L.; Robert, M.; Savéant, J.-M. *J. Am. Chem. Soc.* **2001**, *123*, 4886.
(6) Pierini, A. B.; Vera, D. M. A. *J. Org. Chem.* **2003**, *68*, 9191.

10.1021/jo060054c CCC: $33.50
Published on Web 07/26/2006

CHART 1

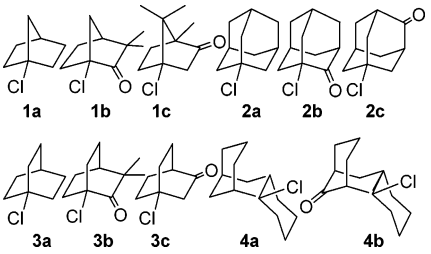

ions)[7a,b] and **2a** > **2c** with $k_{2a} = 2.4 \times k_{2c}$ against Ph_2P^- and $k_{2a} = 5.3 \times k_{2c}$ against Me_3Sn^-.[7c]

The increased reactivity of π-substituted versus unsubstituted alkyl halides in ET-catalyzed nucleophilic substitutions ($S_{RN}1$) has been explained, within the stepwise scheme, by an intramolecular π catalysis.[7] In this mechanism, the radicals formed ($R^{\cdot}$) couple with the anionic nucleophile Nu^- to afford $RNu^{-\cdot}$ (Nu = PPh_2, $SnMe_3$). The ET from this intermediate to a pair of RXs is the key step to propagate the cyclic mechanism and has been shown to determine the relative reactivity of the RX pair.[8a] Thus, a π-substituent lowers the electron affinity of RX, enhancing the intermolecular ET (Figure 1a, [e] = $RNu^{-\cdot}$), the cleavage to $R^{\cdot}$ being favored when this ET is followed by an effective intra-DET (Figure 1a).

A catalytic effect could also be explained within the dissociative-concerted framework. For example, the reductive cleavage of neophyl chloride ((2-chloro-1,1-dimethylethyl)benzene, **5**), which has an anionic curve without any RA minimum, is almost 1 order of magnitude faster than that of neopentyl chloride **6**.[8a] The strong delocalization between the phenyl π system and the σ^*C−Cl through the neopentyl bridge and the further stabilization of the radical formed due to the phenyl substitution lead to an overall stabilization of the anionic curve of **5** with respect to **6** and are responsible for its increased reactivity. [8b]

On the bases presented, the reductive cleavage of compounds **1**−**3** will be explored by theoretical means and their reactivity inspected under both the dissociative-concerted and the stepwise mechanistic paths.

The schematic anionic potential energy surfaces (PES) profile for the carbonyl derivatives **1c**, **2c**, and **3b**,**c** (no methyl substituted) along the bond-breaking coordinate are shown in the gas phase and in solution in Figure 2a and b, respectively. The main thermodynamic magnitudes presented in Table 1 are indicated in Figure 2. In the gas phase, the ground anionic state of these compounds smoothly transforms from π to σ along a quasi-dissociative exothermic path at both the BPW91/ and the PBE/6-31+G* levels with a very low or no barrier (0.3−0 kcal/mol). The profiles with B3LYP were similar except that the π RAs are more shoulder-like and could not be characterized as a minimum for most carbonyl species.

In contrast to the gas-phase profile, the incorporation of a polar solvent sensibly stabilizes the π region and a true π RA minimum appears on this surface for **1c**, **2c**, **3c**, and **3b** as shown in Figure 2. As can be seen from the electrostatic potential map presented in Figure 3a for the RA of **2c** as representative, in the gas phase there exists a strong coupling between the carbonyl π system, the alkyl bridge, and the σ^*(C−Cl), which results in the delocalization of the charge and the spin density preventing

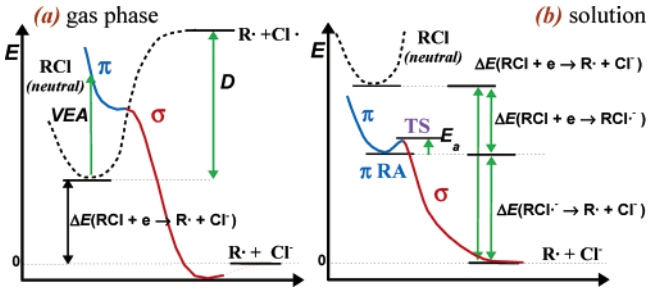

FIGURE 2. Schematic profiles of the calculated anionic curves (solid) in (a) gas phase and (b) in solution for **1c**, **2c**, and **3b**,**c**. Magnitudes summarized in Table 1 are indicated in green. Dashed lines represent the C−Cl dissociation of the neutrals.

TABLE 1. Summary of Results for Carbonyl-Bridgehead Alkyl Halides and Their Anionic and Radical Species[a]

	1b	1c	2b	2c	3b	3c	4b
VEA[b]	−0.49	−0.51	−0.56	−0.44	−0.56	−0.60	−0.40
Δ*E*(RCl + e → RCl·⁻)		−43.58		−41.09	−39.43	−38.75	
D = Δ*E*(RCl → R· + Cl·)	89.15	88.04	82.95	88.04	84.43	79.52	77.45
D, unsubstituted[c]	90.52		85.81		86.76		79.44
Δ*E*(RCl + e → R· + Cl⁻)	−71.66	−72.77	−77.86	−76.64	−76.38	−81.29	−83.36
Δ*E*(RCl + e → R· + Cl⁻)unsubs.[c]	−70.29		−75.00		−74.06		−81.37
E_a		1.20		2.95	0.62	1.02	
Δ*E*(RCl·⁻ → R· + Cl⁻)		−26.97		−33.08	−34.61	−34.73	
RA properties:							
r(C−Cl)[d]		1.940		1.903	1.855	1.855	
q(O)[e]		−0.814		−0.814	−1.013	−1.033	
q(Cl)[e]		−0.404		−0.341	−0.311	−0.321	
spin(C(O))[f]		0.610		0.704	0.699	0.721	
transition state:							
r(C−Cl)[d]		1.981		1.999	1.872	1.881	
q(O)[e]		−0.803		−0.667	−1.005	−1.034	
q(Cl)[e]		−0.451		−1.043	−0.350	−0.313	
radical formed:							
spin(C·)[f]	0.922	0.926	0.934	0.898	0.953	0.931	0.836
s character C·[g]	18.56%	18.04%	13.47%	12.31%	14.50%	16.44%	2.30%
$\hat{a}$[h]	105.7	107.1	112.3	113.5	111.7	112.4	118.0

[a] BPW91/6-31+G* in methanol unless indicated. See also Figure 2. Energies in kcal/mol, except for part (b). [b] VEA (gas-phase vertical electron affinity) in eV. [c] The same magnitude for the carbonyl unsubstituted halides **1a**, **2a**, **3a**, and **4a**, respectively. [d] Bond lengths in angstroms. [e] Electrostatic potential fit charges. [f] Natural spin population (NBO analysis) in au. [g] In the hybridization of the orbital holding the unpaired electron (NBO). [h] Average of the three C<C_{ipso}<C angles in degrees (should be 120° for an unstrained sp^2 radical).

the formation of a stable carbonyl RA. A polar media, on the other hand, strongly stabilizes the localization of the charge on oxygen (C=O). This results in the formation of a solvated RA minimum (Figure 3b), early along the reaction path [*r*(C−Cl) = 1.94 Å, Table 1]. For this system, both the π (C−Cl length similar to the neutral, charge strongly localized on oxygen) and the σ (longer C−Cl length, charge on the halide anion) regions of the curves are stabilized to a greater extent than at intermediate C−Cl lengths, where the anion has a mixed π−σ character. This profile differs from the one shown by the haloaromatic[6] and π-substituted haloaliphatic compounds[8b] previously studied, for which the π RAs and transition state structures (charge delocalized over several centers in both cases) have solvation energies similar among them and much smaller than the σ species (charge in one center, the halide anion).

Considering the changes in the topology of the curves from the gas phase to solution, which have also been observed in related systems,[9] all of the profiles discussed and the magnitudes in Table 1 refer to the BPW91/6-31+G* level with full geometry optimization within methanol as solvent, except for electron affinities (*VEA*) and bond dissociation energies (*D*), which are

(7) (a) Lukach, A. E.; Morris, D. G.; Santiago, A. N.; Rossi, R. A. *J. Org. Chem.* **1995**, *60*, 1000. (b) Santiago, A. N.; Takeuchi, K.; Ohga, Y.; Nishida, M.; Rossi, R. A. *J. Org. Chem.* **1991**, *56*, 1581. (c) Toledo, C.; Santiago, A. N.; Rossi, R. A. *J. Org. Chem.* **2002**, *67*, 2494.

(8) (a) Duca, J. S.; Gallego, M. H.; Pierini, A. B.; Rossi, R. A. *J. Org. Chem.* **1999**, *64*, 2626. (b) Vera, D. M. A.; Pierini, A. B. *J. Phys. Org. Chem.* **2002**, *15*, 894.

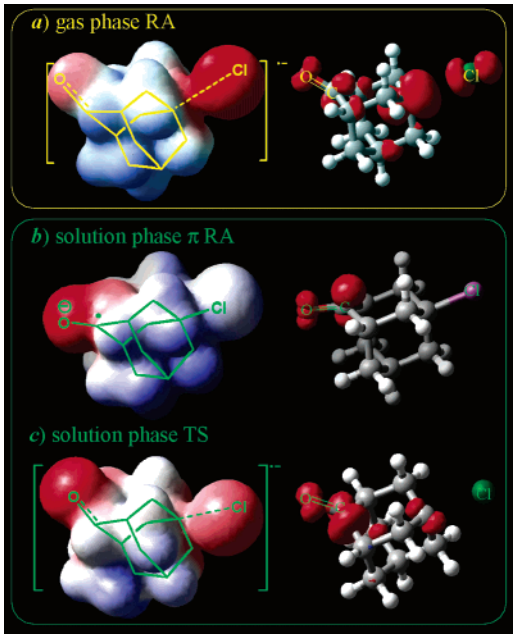

FIGURE 3. Electrostatic potential (left; from blue = positive to red = negative) and spin density (right) on the indicated points along the reaction path for **2c**$^{\cdot -}$, taken as representative.

referred to the gas phase as usual. This functional was chosen due to its smaller computational cost, especially for systems that have to be completely modeled in solvent (B3LYP gas-phase results on selected systems were compared to PBE and BPW91, with a reasonable agreement; see Supporting Information).

On the other hand, PMP2,[8b] QCISD(T),[9] CCSD(T),[6] CASSCF,[6] for related (halo and carbonyl) systems, and preliminary PMP2[10] results for this system, show a profile similar to the DFT methods, indicating that the latter appropriately describe the dissociation of these species. It is clear that the solvent effect with complete geometry optimization must be included to obtain a more appropriate description in solution although some dynamical and discrete effects that contribute to the solvent reorganization energy are not considered in the continuum model.[11] The role of the different bridge paths that connect the π-carbonyl and the σ*C−Cl subsystems was inspected and separated by means of a NBO analysis[12] for **1b**, **1c**, and **2c**. The direct interaction between the C═O and C−Cl NBOs (through space interaction) is almost negligible except for the case of **1b**, in which the subsystems are separated by one C−C bond. In all of the cases, the role of the whole bridge (i.e., considering the contribution of all possible paths) is by far more important, in allowing for the through bond coupling, than the shortest path (minimum number of C−C bonds connecting the C−Cl and

(9) Costentin, C.; Robert, M.; Savéant, J.-M. *J. Am. Chem. Soc.* **2004**, *126*, 16834 and refs cited therein.

(10) Pierini, A. B.; Santiago, A. N.; Allende, S. G.; Vera, D. M. A. *Arkivoc* **2003**, *X*, 477.

(11) Within this approach, at any point in the path the solvent polarization is instantaneously consistent with the solute. The real time scale of the reorganization as well as most discrete effects, as hydrogen-bond formation/depletion, escape to the scope of the model. In organic solvents of dielectric constant around 35, the latter effects are not as critical as in aqueous solution. See also ref 9.

(12) Monitoring the natural charge, spin densities, and orbital energies before and after the appropriate deletions, that is, comparing the real RA with a system in which certain interactions between localized orbitals are not allowed by setting their nondiagonal Fock matrix elements to zero (for details, see Supporting Information).

CHART 2

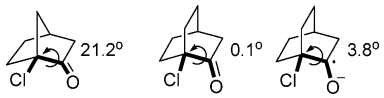

C−O bonds). As a consequence, the overall effect (through space and through bond interactions) is similar for species with the substituents in α, β, and γ, it being slightly weaker for the adamantyl derivative **2c**. The analysis of the anionic PES scan for **1c**, **2c**, and **3b**,**c** (Figure 2) by monitoring the charge and spin distribution (see Figure 3b,c) shows that the π species gradually becomes σ along an adiabatic path. The normal mode corresponding to the intrinsic reaction path involves, besides the trivial C−Cl stretching, an important distortion of the ring, which approaches the $C_{carbonyl}$ and the C_{Cl} centers, the frequency of the TS mode and the height of the barrier being clearly affected by the structural rigidity of the different bridges.

In the α-carbonyl derivatives, the twisting of the C═O and C−Cl by bending of the Cl<C_{ipso}<$C_{carbonyl}$<O (Chart 2) dihedral also allows for a strong direct coupling as the reaction proceeds. Thus, the α-substituted compounds **1b** and **2b** (for which the through space interaction is appreciable) have no characterizable barrier for dissociation and **3b** has the lowest E_a found (<1 kcal/mol). The appearance of this small barrier in **3b** could be ascribed to the geometry of the [2.2.2] bicycle, which enforces the C═O and the C−Cl groups to be almost planar in the RA, precluding the $\pi-\sigma$ direct coupling (see Chart 2).

The β-oxo derivatives **1c** and **3c** dissociate with similar E_a's (∼1 kcal/mol), while the highest E_a is determined for the γ-oxo adamantyl **2c** (∼3 kcal/mol) for which the through bond interaction is slightly weaker. However, this barrier is mainly attributed not to the number of σ-bonds that separates both centers but to the rigidity of the adamantyl bridge that disfavors the transition mode.

While the flexibility of the whole polycycle plays an important role in lowering the barrier for the fragmentation of the RA, the energy of the σ-anionic surface (and then the thermodynamic stability of the products R$^{\cdot}$ + Cl$^-$) does not directly depend on the structural flexibility of the bridge skeleton but on the strain of the C_{ipso} center of the radical formed. The departure from the planarity (reflected on $\hat{a}$, the average C<C_{ipso}<C angle, Table 1), which prevents the formation of a stabilized 2p radical center, reflects on the NBO % s character of the orbital holding the lone electron (i.e., ideally, an unstrained sp^2 radical center should have an $\hat{a}$ = 120° and a 0% s character in that orbital). Moreover, the NBO natural spin at the radical center gives an estimation of its hyperconjugative interactions with the vicinal σ* (C−C) orbitals of the bridge. As can be seen from Table 1, the edges of the trend are the norbornyl derivatives **1**, which have to accommodate the unpaired electron in a practically sp^3 center ($\hat{a}$ of 105−107° (**1a**−**c**)), and the flexible bridgehead species **4b**, which can easily distort to form an almost 2p radical. A similar trend is observed in the stability of the carbonyl-unsubstituted derivatives. On the other hand, the adamantyl moiety despite being the most rigid bridge affords the less strained radical.

According to the Savéant theory for concerted-dissociative ET (Figure 1b),[1,5] the rate of the cleavage will be controlled by the exergodicity of RCl + e → R$^{\cdot}$ + Cl$^-$, which depends on intrinsic factors, mainly the bond dissociation energy, which, for the same leaving group, reflects on the stability of the radical formed and on the solvent reorganization energy. The relative energy of the anionic σ-surface with respect to the neutral gives information of the first of these factors, which can be identified

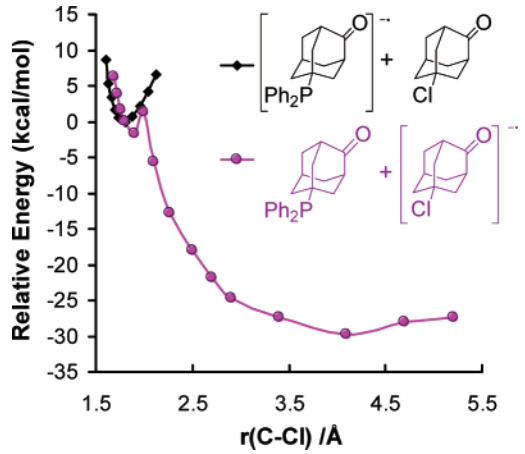

FIGURE 4. Neutral and anionic profiles of **2c**, corrected by the driving force of the donor in solution.

as ΔE(RCl + e → R˙ + Cl⁻) in Table 1 for comparing reactions against the same donor (D˙⁻ → D + e, i.e., given the same $\Delta G_{D\cdot-/D}{}^{0}$).

Based on our calculations, the concerted-dissociative pathway will be followed by **1b**, **2b**, and **4b** (no RA on the anionic surfaces) as well as for the trivial case of the unsubstituted halides. Even though the carbonyl and the C−Cl are in β in **4b**, the intermediacy of a RA is discarded. This compound has the highest flexibility, and it affords a remarkably stable radical upon dissociation, and so it has the most exothermic and dissociative character (no experimental data are available for these compounds).

Assuming this concerted-dissociative pathway, **1b**, for example, should fragment faster than **1a** [ΔE(RCl + e → R˙ + Cl⁻) = −71.66 against −70.29 kcal/mol, Table 1], in agreement with the experimental reactivity. However, **1c** (−72.77) and **3b** (−76.38) would be more reactive than **1b**. In fact, **1c** and **3b** could form a RA, following a different profile than **1b**, even though their RAs have considerably small E_a's. Moreover, the barriers could increase in a discrete solvent simulation,[9] and, on the other hand, even a small E_a could play a role in the experimental conditions (liquid ammonia, −33 °C).

Similarly, **2c** should be more reactive than the unsubstituted **2a** (ΔE −76.6 vs −75.0), opposed to the experimental observation.[7c] On these bases, the formation of the RA of **2c** seems the only pathway consistent with the experimental data. For an additional test for this hypothesis, we also estimated the driving force of the overall reaction for **2c**, by adding the energy of the donor (RNu˙⁻) to the neutral curve and the energy of the oxidized donor (RNu) to the anionic curve. The results are shown in Figure 4 for the poorer electron donor, R−PPh$_2$˙⁻, which gives a driving force high enough for reaching the RA energy, favoring a stepwise path (see also Supporting Information for SnMe$_3$⁻ as nucleophile).

It is concluded that, besides the relative position of the substituent (in α, β, or γ), the rate of an intra-DET in RAs of the **1**−**3** family is strongly influenced by the flexibility of the bridge. The energetics of both the RA fragmentation and the concerted-dissociative cleavage of the halides are sensitive to the stability of the radical formed. This factor closely relates to the structural nature of the bridge, particularly to its ability for rearranging to a sp^2 center.

The stepwise path, with the intermediacy of a RA, would have a relative importance in the case of **1c** and **3b** against **1b**. In the adamantane family, the experimental reactivity of **2c** against the unsubstituted **2a** could be explained by a stepwise mechanism for **2c** and the concerted-dissociative cleavage of **2a**.

Computational Procedures

The calculations were performed with the Gaussian 03[13a] and Jaguar 5.016[13b] packages. The characterization of stationary points was done as usual by Hessian matrix calculations. The exploration of the potential surface was carried out within the gradient generalized, pure PBE[14] and BPW91[15] DFT[16] functionals and the hybrid B3LYP[17] varying the selected coordinate with full optimization for the remainder degrees of freedom. In all cases, the spin contamination along the whole fragmentation paths was negligible. The zero-point energy corrections were made at the 6-31+G* level for the D and ΔE's thermodynamic quantities. The energies in solution were obtained with full geometry optimization in the continuum solvent (model solvent methanol: dielectric constant = 33.7, density = 0.7914 g/mL) using Jaguar.[18] The general procedure for exploring the neutral and anionic surfaces was similar to that applied to $\pi-\sigma$ adjacent systems, and proved to be reliable enough to accurately predict thermodynamics and electron/molecule properties.[6,8b] The halides **1**−**4** have negative electron affinities (*VEA*); for these species the conventional valence[19] anion state has been characterized as the RA. The basis sets and methodologies have been already tested and expected to yield the right anion state, reproducing *VEA*s within a few tenths of eV.[6,19] The natural bond orbitals (NBO) theory has been applied to qualitatively understand and dissect the contributions to the interaction between the π*, the bridge, and the σ*C−Cl systems, using the programs NBO 3.2 and 5 built within Gaussian and Jaguar, respectively.[20]

Acknowledgment. This work was supported by the Agencia Córdoba Ciencia, the Consejo Nacional de Investigaciones Científicas y Técnicas (CONICET), SECYT, Universidad Nacional de Córdoba, Argentina.

Supporting Information Available: Part 1: The *xyz* coordinates of the species calculated. Part 2. (A) Total energies (au) and details about the oxo unsubstituted derivatives. (B) Results for the gas-phase PES, as well as B3LYP and PBE functional results for selected systems with 6-31+G* and 6-311+G(2df,p) basis sets. (C) Details about the driving force estimation. (D) NBO analysis details. This material is available free of charge via the Internet at http://pubs.acs.org.

JO060054C

(13) (a) http://www.gaussian.com. (b) http://www.schrodinger.com.
(14) (a) Perdew, J. P.; Burke, K.; Ernzerhof, M. *Phys. Rev. Lett.* **1996**, *77*, 3865. (b) Perdew, J. P.; Burke, K.; Ernzerhof, M. *Phys. Rev. Lett.* **1997**, *78*, 1396.
(15) (a) Burke, K.; Perdew, J. P.; Wang, Y. In *Electronic Density Functional Theory: Recent Progress and New Directions*; Dobson, J. F., Vignale, G., Das, M. P., Eds.; Plenum: New York, 1998. (b) Perdew, J. P.; Wang, Y. *Phys. Rev. B* **1992**, *45*, 13244.
(16) Kohn, W.; Sham, I. *J. Phys. Rev.* **1965**, *140*, A1133.
(17) (a) Lee, C.; Yang, W.; Parr, R. G. *Phys. Rev. B* **1988**, *37*, 785. (b) Becke, A. D. *Phys. Rev. A* **1988**, *38*, 3098. (c) Miehlich, B.; Savin, A.; Stoll, H.; Preuss, H. *Chem. Phys. Lett.* **1989**, *157*, 200.
(18) (a) Tannor, D. J.; Marten, B.; Murphy, R.; Friesner, R. A.; Sitkoff, D.; Nicholls, A.; Ringnalda, M.; Goddard, W. A.; Honig, B. *J. Am. Chem. Soc*. **1994**, *116*, 11875. (b) Marten, B. K.; Cortis, C.; Friesner, R. A.; Murphy, R. B.; Ringnalda, M.; Sitkoff, D.; Honig, B. *J. Phys. Chem*. **1996**, *100*, 11775.
(19) Vera, D. M. A.; Pierini, A. B. *Phys. Chem. Chem. Phys.* **2004**, *6*, 2899 and literature cited therein.
(20) (a) Carpenter, J. E. Ph.D. Thesis, University of Wisconsin, Madison, WI, 1987. (b) Carpenter, J. E.; Weinhold, F. *J. Mol. Struct. (THEOCHEM)* **1988**, *169*, 41. Program NBO 3.2: Glendering, E. D.; Reed, A. E.; Carpenter, J. E.; Weinhold, F., University of Wisconsin.